IL NUOVO CIMENTO **45 C** (2022) 65
DOI 10.1393/ncc/i2022-22065-0

Communications: SIF Congress 2021

Study of strangeness production in pp collisions as a function of multiplicity and effective energy with ALICE

F. Ercolessi for the ALICE Collaboration
INFN e Università di Bologna - Bologna, Italy

received 31 January 2022

Summary. — The study of energy and multiplicity dependence of strange hadron production in proton-proton collisions provides a powerful tool to understand similarities and differences between small and large collision systems. In these proceedings, recent ALICE preliminary results are presented, which contribute to a better understanding of the strangeness production in pp collisions at $\sqrt{s} = 13\,\text{TeV}$. Multi-strange Ξ^- and $\overline{\Xi}^+$ baryon yields are studied as a function of multiplicity and effective energy, *i.e.*, the energy available for particle production in the event. The main novelty of this analysis is the introduction of a new effective energy estimator, which is based on the energy deposited in ALICE Zero Degree Calorimeters. Such a multi-differential approach allows disentangling initial and final-state effects in the strangeness production in pp collisions.

1. – Introduction

Strange hadron production in heavy-ion collisions is a crucial observable to investigate the strongly interacting medium created in the interaction. Strangeness enhancement, *i.e.*, the increase in strange hadron production relative to non-strange hadrons, was one of the first proposed signatures of quark-gluon plasma (QGP) formation [1]. This enhancement was observed in heavy-ion collisions at SPS [2], RHIC [3] and LHC [4] at increasing collision energies and follows a hierarchy related to the strangeness content of the particle, being higher for multi-strange hadrons. The ALICE experiment has also studied strangeness production in small collision systems, such as proton-proton, by measuring the ratio of strange particle yields to pion yields as a function of the charged-particle multiplicity produced in the event [5,6]. A summary of ALICE results in large and small collision systems is shown in fig. 1. The ratio to pions is found to increase with multiplicity, evolving smoothly across different collision systems and energies. This behaviour is striking as different particle production mechanisms are expected to be involved in the different collision systems. The data are compared to different phenomenological models, from a statistical hadronization description using the canonical suppression approach [7], to rope hadronization models including colour reconnection effects [8], to two-component

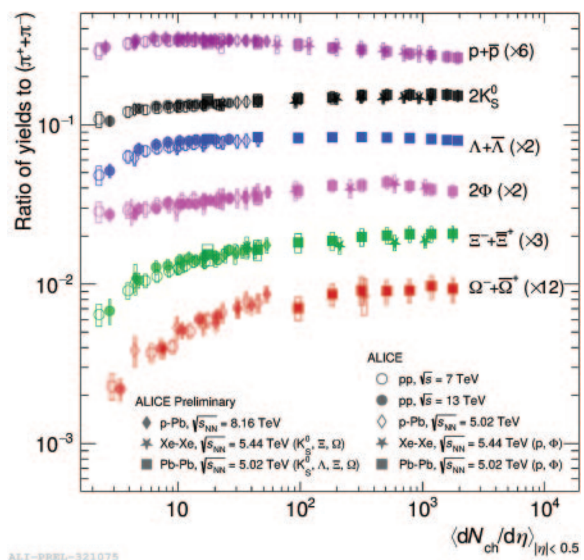

Fig. 1. – Ratio of different strange particle yields to pion yields as a function of the charged-particle multiplicity produced in the event for different collision systems and energies.

(core-corona) models [9]. However, the observed behaviour cannot be satisfactorily reproduced by any of the available models. Further developments are needed to obtain a complete microscopic understanding of strangeness production in hadronic collisions.

The multiplicity distribution of charged particles produced in pp collisions is a characteristic of the final state of the hadronic interaction. However, it also provides important information on its initial dynamics being strongly correlated with the energy effectively available for particle production in the initial stages of the interaction (effective energy). In pp collisions, the effective energy is reduced with respect to the full centre-of-mass energy due to the so-called "leading baryon effect". This effect is related to the quantum number flow conservation and consists in a high probability to emit baryons at forward rapidity, *i.e.*, with large longitudinal momenta along the direction of the incident beams. These forward emitted particles carry away a fraction of the incident primary energy and therefore reduce the effective energy available for particle production. This observable was first used in experiments done at the ISR [10-13]. The ALICE Zero Degree Calorimeters (ZDC) [14], composed of two sets of hadronic calorimeters placed at very forward rapidities on each side of the interaction point, are able to detect the energy deposits of these leading baryons in each event hemisphere and allow estimating the effective energy on an event-by-event basis as $E_{\text{effective}} = \sqrt{s} - E_{\text{leading}}$ [15]. In these proceedings, the production of primary multi-strange Ξ^- and $\overline{\Xi}^+$ baryons is studied as a function of effective energy and multiplicity, in order to investigate the role of initial and final state effects on strangeness enhancement in pp collisions.

2. – Experimental setup and data sample

A detailed description of the ALICE apparatus and its performance can be found in [16]. In this section, the main detectors used for the measurements presented in these proceedings are briefly described. The ALICE detector is composed of a central barrel, which covers the pseudorapidity region $|\eta| < 0.9$ and is devoted to vertex reconstruction, tracking and charged particle identification, complemented by specialised forward detectors. The main detectors involved in strange hadron identification are the six-layer high resolution Inner Tracking System (ITS) [17, 18] and the large volume Time Projection Chamber (TPC) [19]. In addition, the Time-Of-Flight detector (TOF) [20] is exploited in combination with the ITS to suppress the out-of-bunch pileup, by requiring that at least one of the daughter tracks of the (multi-)strange hadron under study gives a signal in one of these detectors. The two innermost layers of the ITS consist of two arrays of Silicon Pixel Detectors (SPD) and are used to measure the average pseudorapidity density of primary charged particles $\mathrm{d}N_{\mathrm{ch}}/\mathrm{d}\eta$ [21]. To study the multiplicity dependence of particle production, the event sample is divided into percentile classes based on the signal amplitude measured by the V0 detectors [22], two sets of plastic scintillators covering the pseudorapidity regions $2.8 < \eta < 5.1$ and $-3.7 < \eta < -1.7$. Effective energy percentile classes are defined studying the distribution of the energy deposits measured by the Zero Degree Calorimeters (ZDC), two sets of hadronic calorimeters, one for protons (ZP) and one for neutrons (ZN) on each side of the interaction point. The ZN are placed at zero degrees relative to the LHC axis, covering the pseudorapidity region $|\eta| > 8.8$. The ZP are placed externally to the outgoing beam pipe on the side where positively charged particles are deflected by the beam optics, in the pseudorapidity region $6.5 < |\eta| < 7.4$. The good capability of the ZDC to estimate the effective energy, measuring the energy deposits of leading baryons, depends on its acceptance and on the limitations related to the beam optics deflection of protons. In ref. [15] a detailed study of the constraints related to the reconstruction of the effective energy in the ZDC and the background from other particles in the forward region is presented, concluding that these effects do not introduce a significant bias in the measurement.

The preliminary results presented in these proceedings are obtained using a data sample collected during the 2015 LHC run with pp collisions at $\sqrt{s} = 13\,\mathrm{TeV}$ and a minimum bias trigger requiring a hit in both V0 scintillators in coincidence with the arrival of proton bunches from both directions. The events are required to have at least one charged particle reconstructed in the pseudorapidity interval $|\eta| < 1$ (INEL > 0([1])) and a reconstructed collision vertex with a position along the beam axis $|z_{vtx}| < 10\,\mathrm{cm}$ with respect to the nominal interaction point.

3. – Analysis details

The ALICE experiment identifies strange baryons ($\Lambda, \bar{\Lambda}, \overline{\Xi}^{+}, \Xi^{-}, \overline{\Omega}^{+}$ and Ω^{-}) via the topological reconstruction of their weak decays in the central pseudorapidity region. A set of geometrical and kinematic selections is applied to the reconstructed candidates in order to identify specific decay topologies to improve the signal/background ratio. Strange hadrons are divided into two topological classes: the V0 topology (Λ baryons), characterized by a V-shaped decay into oppositely charged particles, and the cascade topology (Ξ^{-}, Ω^{-} and their antiparticles), which requires the reconstruction of an additional charged track. The decay channels used to reconstruct strange baryons with ALICE are summarized in table I.

The Ξ^{-} and $\overline{\Xi}^{+}$ baryon raw signal yields were extracted from fits to the candidates invariant mass distributions in different p_{T} intervals. The mass distributions were fitted

([1]) INEL > 0 is a conventional event class which contains events with at least one charged particle in $|\eta| < 1$.

TABLE I. – *Weak decay channels and corresponding branching ratio (B.R.) used to identify* Λ, $\bar{\Lambda}$, $\overline{\Xi}^{+}$, Ξ^{-}, $\overline{\Omega}^{+}$ *and* Ω^{-} *baryons with ALICE* [23].

Particle	Decay channel	B.R. (%)
Λ (uds)	$\Lambda \rightarrow p + \pi^{-}$	63.9 ± 0.5
$\bar{\Lambda}$ ($\bar{\mathrm{u}}\bar{\mathrm{d}}\bar{\mathrm{s}}$)	$\bar{\Lambda} \rightarrow \bar{\mathrm{p}} + \pi^{+}$	63.9 ± 0.5
Ξ^{-} (dss)	$\Xi^{-} \rightarrow \Lambda + \pi^{-}$	99.887 ± 0.035
$\overline{\Xi}^{+}$ ($\bar{\mathrm{d}}\bar{\mathrm{s}}\bar{\mathrm{s}}$)	$\overline{\Xi}^{+} \rightarrow \bar{\Lambda} + \pi^{+}$	99.887 ± 0.035
Ω^{-} (sss)	$\Omega^{-} \rightarrow \Lambda + K^{-}$	67.8 ± 0.7
$\overline{\Omega}^{+}$ ($\bar{\mathrm{s}}\bar{\mathrm{s}}\bar{\mathrm{s}}$)	$\overline{\Omega}^{+} \rightarrow \bar{\Lambda} + K^{+}$	67.8 ± 0.7

with a Gaussian function, for modelling the signal, and a linear function to model the background. The peak region is defined within $\pm\, 4\sigma$ with respect to the Gaussian mean extracted in each p_{T} bin, being σ the standard deviation of the Gaussian function. Adjacent background bands, covering a mass interval as wide as the peak region (4σ), are defined on both sides. The signal is then extracted integrating the background-subtracted mass distribution in the peak region. The raw yields in p_{T} intervals are then corrected for acceptance and efficiency using Monte Carlo simulations. Events are generated using the PYTHIA 6.425 (Tune Perugia 2011) generator [24, 25] and transported using GEANT 3 [26] (v2-01-1) which simulates the passage of particles through the experimental apparatus. The p_{T}-integrated yields are extracted from the corrected p_{T}-spectra which are extrapolated to the unmeasured p_{T} intervals based on a fit with a Tsallis-Lévy parametrization [27]. The study of systematic uncertainties follows the analysis described in [6].

4. – Results

The ALICE Collaboration has measured that the forward energy detected by the ZDC and the charged-particle multiplicity produced at midrapidity are anti-correlated [28]. This relation is further studied in this analysis using the PYTHIA 8 event generator and displayed in fig. 2. The simulated events are categorized into V0 multiplicity and ZDC energy([2]) classes with the same approach used for the raw data analysis, which was described in sect. **2**. The results from PYTHIA8 simulations show that events selected using a V0 or ZDC based estimator are sensitive to both initial and final state, *i.e.* to the effective energy and to the charged particle multiplicity. Figure 3 displays the ratio of $\Xi^{-} + \overline{\Xi}^{+}$ yields to the charged-particle multiplicity in the event (self-normalized to the same ratio in INEL > 0 events) as a function of the average pseudorapidity density of primary charged particles ($\mathrm{d}N_{\mathrm{ch}}/\mathrm{d}\eta$), which is measured with the SPD. Two sets of data points are shown, selected based on the multiplicity percentile measured by V0 and effective energy percentile measured by ZDC. The $\Xi^{-} + \overline{\Xi}^{+}$ production is found to increase with

([2]) The ZDC-based percentile estimator is labelled as $\sqrt{s}-$ZDC and it represents the percentile classes of the quantity $\sqrt{s} - E_{\mathrm{ZDC}}$.

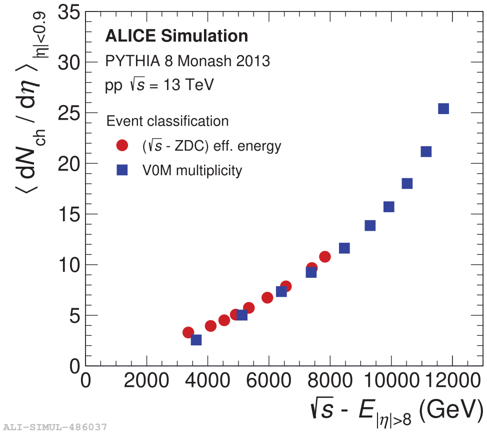

Fig. 2. – Multiplicity and effective energy correlation in PYTHIA 8 using V0 (blue squares) and ZDC (red circles) event classes. See text for more details.

multiplicity following a continuous trend, independent of the estimator.

To decouple initial and final state effects, strangeness production is studied double differentially, *i.e.*, in intervals of effective energy and multiplicity. In particular, events are selected using ZDC percentile selections, by fixing the multiplicity through the V0 estimator in a high and a low range (red full and open circles), and vice-versa using V0 percentile selections, by fixing the effective energy through the ZDC estimator to a high and a low range (blue full and open squares). Figure 4(a) shows the ratio of $\Xi^- + \overline{\Xi}^+$ yields to the average charged-particle multiplicity as a function of effective energy for two multiplicity classes selected using the V0 signals. As it is evident from the observed trend, $\Xi^- + \overline{\Xi}^+$ production is independent of effective energy. A larger yield is observed for events with higher multiplicity, as expected. This conclusion is confirmed by the observed trend of $\Xi^- + \overline{\Xi}^+$ production as a function of multiplicity for different effective energy classes shown in fig. 4(b).

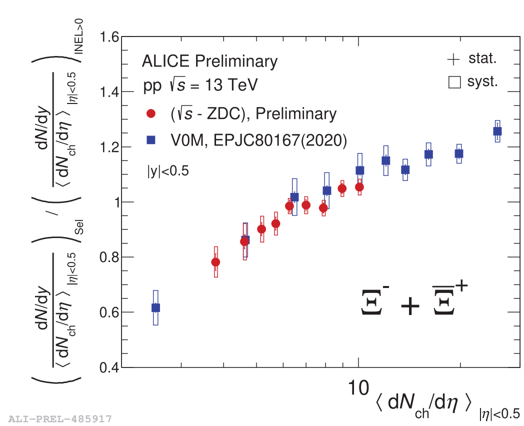

Fig. 3. – Ratio of $\Xi^- + \overline{\Xi}^+$ yields to the charged-particle multiplicity (self-normalized to INEL > 0) as a function of charged-particle pseudorapidity density at midrapidity, using V0 (blue squares) and ZDC (red circles) standalone selections.

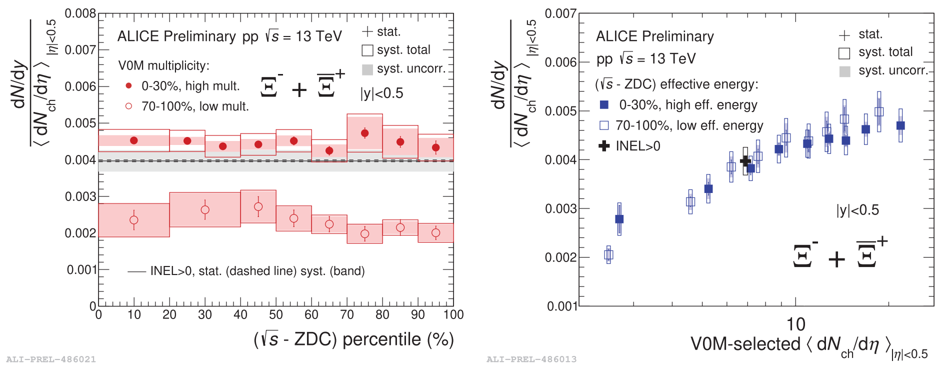

Fig. 4. – Ratio of $\Xi^- + \overline{\Xi}^+$ yields to the charged-particle multiplicity extracted using V0-ZDC combined selections. (a) Events are selected using ZDC event classes, fixing the multiplicity through the V0 estimator. (b) Events are selected using V0 event classes, fixing the effective energy through the ZDC estimator.

These preliminary results suggest that the effective energy does not play a significant role in the strangeness enhancement observed in pp collisions, confirming a strong role of the final state multiplicity.

5. – Conclusion

The ALICE Collaboration has provided a comprehensive set of results on the production of strange hadrons in pp collisions, which show a striking smooth trend with increasing multiplicity from pp to heavy-ion. However, the observed behaviour cannot be quantitatively reproduced by the existing models and commonly used event generators and the mechanisms responsible of this intriguing effect are still unclear. The set of preliminary results presented in these proceedings exploit a multi-differential approach to study strange hadron production in pp collisions at $\sqrt{s} = 13\,\text{TeV}$. The main feature of this analysis is the introduction of a new effective energy estimator, based on the information provided by the Zero Degree Calorimeters. This new estimator, combined with the multiplicity one, provides a novel sensitivity to the initial and final stages of the collision in the study of particle production. The results might confirm that the strangeness enhancement in pp interactions is connected to the final particle multiplicity produced in the collision and suggest no significant dependence on the initial effective energy. Future studies in the ALICE experiment will explore more differential event classes to further investigate the dependence of strangeness production on the initial and final phases of the collision. For this purpose, new energy and multiplicity estimators are being tested.

REFERENCES

[1] Rafelski J. and Müller B., *Phys. Rev. Lett.*, **48** (1982) 1066.
[2] The WA97 Collaboration, *Phys. Lett. B*, **449** (1999) 401.
[3] STAR Collaboration (Agakishiev G. *et al.*), *Phys. Rev. Lett.*, **108** (2012) 072301.
[4] ALICE Collaboration, *Phys. Lett. B*, **728** (2014) 216.
[5] ALICE Collaboration, *Nat. Phys.*, **13** (2017) 535.
[6] ALICE Collaboration, *Eur. Phys. J. C*, **80** (2020) 167.

[7] Vovchenko V. *et al.*, *Phys. Rev. C*, **100** (2019) 054906.
[8] Nayak R. *et al.*, *Phys. Rev. D*, **100** (2019) 074023.
[9] Kanakubo Y. *et al.*, *Phys. Rev. C*, **101** (2020) 024912.
[10] Basile M. *et al.*, *Phys. Lett. B*, **92** (1980) 367.
[11] Basile M. *et al.*, *Phys. Lett. B*, **95** (1980) 311.
[12] Basile M. *et al.*, *Nuovo Cimento A*, **67** (1982) 244.
[13] Basile M. *et al.*, *Nuovo Cimento A*, **79** (1984) 1.
[14] ALICE Collaboration, *Nucl. Instrum. Methods A*, **581** (2007) 397.
[15] Akindinov A. *et al.*, *Eur. Phys. J. C*, **50** (2007) 341.
[16] ALICE Collaboration, *JINST*, **3** (2008) S08002.
[17] ALICE Collaboration, *JINST*, **5** (2010) P03003.
[18] ALICE Collaboration, *J. Phys. G*, **41** (2014) 087002.
[19] ALICE Collaboration, *Nucl. Instrum. Methods A*, **622** (2010) 316.
[20] ALICE Collaboration, *Eur. Phys. J. Plus*, **128** (2013) 44.
[21] ALICE Collaboration, *Phys. Rev. Lett.*, **110** (2013) 032301.
[22] ALICE Collaboration, *JINST*, **8** (2013) P10016.
[23] Particle Data Group (Tanabashi M. *et al.*), *Phys. Rev. D*, **98** (2018) 030001.
[24] Sjöstrand T., Mrenna S. and Skands P. Z., *JHEP*, **05** (2006) 026.
[25] Skands P. Z., *Phys. Rev. D*, **82** (2010) 074018.
[26] Brun R., Bruyant F., Carminati F., Giani S., Maire M., McPherson A., Patrick G. and Urban L., *GEANT: Detector Description and Simulation Tool* (CERN-W5013) 1993, `https://doi.org/10.17181/CERN.MUHF.DMJ1`.
[27] ALICE Collaboration, *Phys. Lett. B*, **728** (2014) 25.
[28] ALICE Collaboration, `https://arxiv.org/abs/2107.10757`.